ECS Transactions, 50 (2) 1815-1822 (2012)
10.1149/05002.1815ecst ©The Electrochemical Society

Nitrogen-doped Activated Graphene Supported Platinum Electrocatalyst for Oxygen Reduction Reaction in PEM Fuel Cells

Ja-Yeon Choi, Dong Un Lee and Zhongwei Chen

Department of Chemical Engineering, University of Waterloo, Waterloo, Ontario, Canada, N2L 3G1

Highly active and durable platinum catalyst was successfully synthesized employing nitrogen-doped activated graphene as a catalyst support material. The physical characterization using XRD and TEM indicates the presence of nitrogen-doping on graphene leads to uniform distribution of Pt nanoparticles and effective formation of active sites exposed for reaction. The electrocatalytic activity for oxygen reduction reaction of Pt/N-AG catalyst was confirmed by half-cell measurement, Accelerated durability test (ADT) was also conducted to investigate the durability of the catalyst by running the half-cell test for 1000 cycles in N2 saturated electrolyte. The catalyst demonstrates superior electrocatalyst activity and durability over Pt/XC72 catalyst for ORR under the studied conditions, rendering graphene as an ideal replacement to traditional nanostructured carbon support materials.

Introduction

Polymer electrolyte membrane (PEM) fuel cells have been viewed as promising power source candidates for transport, stationary, and portable applications due to their high efficiency and low emissions(1). The platinum is the most commonly used catalyst material for the oxygen reduction reaction (ORR) at the cathode of PEM fuel cells; however, the limited abundance and high cost of platinum hinder the large-scale commercialization of fuel cells(2-4). To overcome this limitation, it is necessary to enhance the catalyst utilization in order to improve the catalytic activity while decreasing its platinum loading.

The material on which the catalyst is supported is important for the high dispersion and narrow distribution of Pt nanoparticles, and these characteristics are closely related to electrocatalytic activity of the catalysts(5). The support materials can influence the catalytic activity by interplaying with catalytic metals, and the durability of the catalyst is also greatly dependent on its support(6). A variety of support materials like carbons, oxides, carbides, and nitrides have been employed as supports materials for Pt(7-12), and much effort has been devoted to the synthesis of the novel carbon supports with large surface area and pore volume, including nanostructured carbons such as carbon nanotubes (CNTs), carbon nanofibers, and mesoporous carbon(13-19). For example, nanostructured carbon supported Pt catalysts have shown improved catalytic activity and durability compared to the commercial catalyst supported on Vulcan XC-72 carbon black, due to the structural and electrical properties of CNTs(20). Mesoporous carbon supported Pt catalysts also have shown excellent performance in PEM fuel cell electrode reactions, attributed to the high uniform dispersion of catalytic metals, the high electrical

conductivity, and the enhanced mass transfer due to the pore structure of the materials(21, 22). The carbon support can also be doped by other atoms or compounds in order to obtain both improved catalytic activity and enhanced durability for ORR(23-25). These novel nanostructured carbon materials have achieved promising performance in terms of catalytic activity and durability. However, there is still enormous demand and potential for the catalysts to improve.

Graphene, consisting of a two-dimensional (2D) monolayer of graphitic carbon atoms, has been viewed as a promising candidate for the fuel cell catalyst support, due to its many intriguing properties such as high aspect ratios, large surface areas, rich electronic states, good electron transport, thermal/chemical stability and good mechanical properties(26, 27). Especially nitrogen-doped graphene has been found to have an excellent electrochemical activity towards ORR even though the real active site and the reaction mechanism of nitrogen-doped species with oxygen are still unclear(28). In this study, we have developed Pt catalyst by combining the precious metal with nitrogen-doped activated graphene (N-AG) as the support. A transmission electron microscopy (TEM) image of the catalyst in Figure 2 shows uniform size and distribution of platinum nanoparticles on a graphene layer. This novel catalyst demonstrates superior electrocatalyst activity and durability over Pt/XC72 catalyst for ORR under the studied conditions, rendering graphene as an ideal replacement to traditional nanostructured carbon support materials.

Experimental

Catalyst Synthesis

The activated graphene (AG) and nitrogen-doped activated graphene (N-AG) was synthesized by thermal shock method(29). Graphene oxide undergoes thermal shock from room temperature to 800°C within five seconds in inert atmosphere in a tube furnace. It has been studied that by rapidly raising the temperature, it maximizes the exfoliation of the GO sheets due to higher diffusion rate of the evolved gases during the decomposition of the oxygen groups in GO than the van der Waals forces holding the GO sheets together. The exfoliated graphene is then soaked in 7 M KOH for 24 hours and filtered, followed by drying in an oven. The powder is once again heated at 900 °C in the tube furnace in inert atmosphere to synthesize activated graphene. Lastly, another heat treatment in the presence of ammonia gas completes the synthesis of nitrogen-doped activated graphene. The activated sample undergoes a rapid heating from room temperature to 800 °C by sliding a long quartz tube containing the sample in the tube furnace and was kept for an hour before it cools down. The nitrogen-doping of exfoliated graphene happens in the presence of ammonia (1:1 ratio of ammonia and argon, each at 50 sccm), which reacts with oxygen groups in GO to form C-N bonds.

The Pt supported on nitrogen doped activated graphene catalyst (Pt/N-AG) was prepared by the polyol method, depositing Pt (20 wt. %) on two types of graphene supports in ethylene glycol solvent under 3 h of heat-treatment at 140 °C. The mixture is then filtered and oven dried overnight. The commercial 20 wt. % platinum on Vulcan XC-72 catalyst (Pt/XC72) was used as a reference in order to compare the effect of having different catalyst support.

Physical Characterization

X-ray diffraction (XRD) data were obtained by using an Inel XRG 3000 with Cu KR radiation to determine the particle size of the platinum nanoparticles. A broad range scan of 2θ from 0.288 ◦ to 113 ◦ was carried out for about 10 min on each sample. Transmission electron microscopy (TEM) was conducted using a Philips CM300 at 300 kV.

Electrocatalytic Activity Evaluation

The electrocatalytic activity was evaluated in a three-electrode electrochemical cell using a Pine-Instrument's Bipotentiostat AFCBP1, equipped with a speed rotator. The electrode was equipped with a 0.19635 cm^2 glassy carbon surface. All RDE measurements were performed in acidic electrolyte, 0.1 M HClO4, using a Ag/AgCl reference electrode at room temperature. To prepare the electrode, 4 mg of sample was dissolved ultrasonically into 2 mL of ethanol before 20 μL of the ink and 10 μL of 0.05% Nafion solution were applied to the glassy carbon disk. The catalyst loading on the glass carbon electrode was approximately 200 μ g/cm^2 which makes 40 μ g/cm^2 Pt loading. ORR curves were recorded in the potential range at a scan rate of 10 mV/s at various rotation speeds (100, 400, 900, and 1600 rpm) with the electrolyte saturated with oxygen gas. ORR curves were corrected for the background by conducting the same sweep voltammetry in the absence of oxygen and subtracting the curve from the measured ORR curves. The accelerated degradation test (ADT) was conducted by running 1000 cycles in the potential range from 0 V to 1.2 V vs RHE at a scan rate of 50 mV/s in nitrogen saturated electrolyte.

Results and Discussion

In order to evaluate the particle size of the Pt particles deposited on both Pt/XC72 and Pt/N-AG, XRD technique was utilized. The mean platinum particle size for the two catalyst materials can be estimated from Scherrer's equation:

$$d = K\lambda / (B * \cos\theta) \quad [1]$$

where d is the particle diameter (nm), K is the shape factor (0.89), λ is the wavelength of the x-rays (0.154 nm), B is the full width at half-maximum (FWHM) of the peak in radian and θ is the Bragg angle in degrees. Figure 1 shows the diffraction patterns of the different catalysts with the platinum peaks at approx. 39◦, 46◦, 67◦, 81◦ and 86◦ corresponding to the (111), (200), (220), (311) and (222) faces of platinum, respectively. Particle size calculations of two catalysts were estimated based on the Pt(220) peak which yielded platinum particle sizes of 2.843 nm and 2.475 nm for Pt/XC72 and Pt/N-AG respectively. The results are summarized in table I.

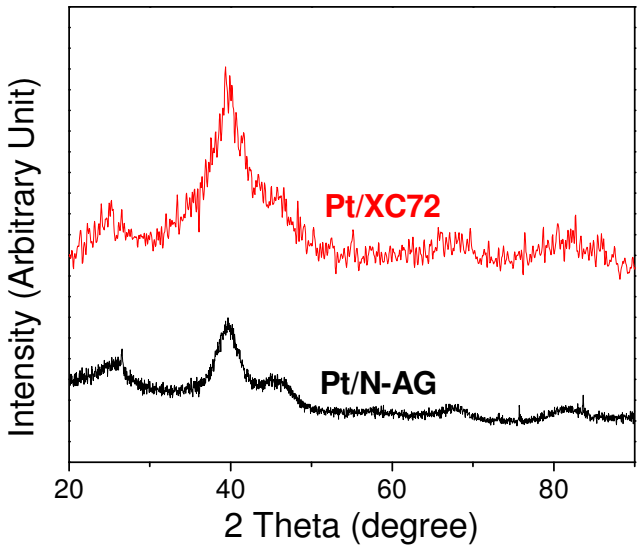

Figure 1. XRD patterns of Pt/XC72 and Pt/N-AG

TABLE I. The mean platinum particle size of Pt/XC72 and Pt/N-AG

	2 theta	FWHM	Diameter (nm)
Pt/XC72	67.287	3.317	2.843
Pt/N-AG	67.408	3.814	2.475

To investigate the surface morphology of graphene support used and to confirm the particle size obtained by XRD, Pt/AG and Pt/N-AG were observed by high resolution TEM, shown in Figure 2. The platinum particles added onto the Pt/N-AG catalyst show better dispersion and reasonably uniform particle sizes than that of Pt/AG. Through TEM, the average particle size of platinum on the Pt/N-AG was approximated to be 3 nm which is in reasonable accordance with XRD data. The wrinkles observed in both catalysts suggest the presence of defects created by activation and/or nitrogen-doping of the graphene. In addition, the TEM image of Pt/AG shows more layered structure of graphene and some of the Pt particles in-trapped between those layers, compared to the single layer and clear Pt particles observed in Pt/N-AG. It seems that presence of nitrogen groups on graphene enhances uniform distribution of Pt nanoparticle as well as reducing the wrinkling effect of the graphene, possibly due to the reduced number of defects upon effective deposition of Pt particles on nitrogen-doped graphene.

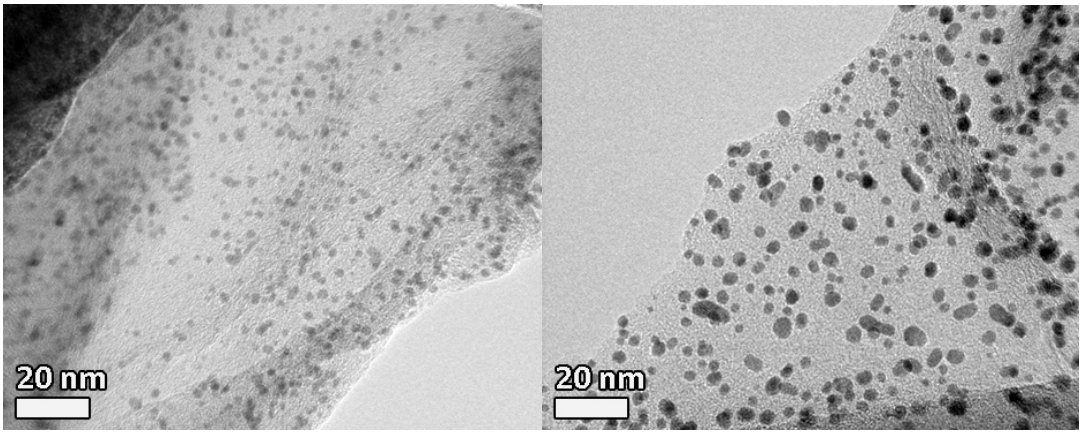

Figure 2. High resolution TEM images of Pt/AG and Pt/N-AG catalysts illustrating Pt nanoparticles and their distribution on the graphene supports

Half-cell RDE experiments were conducted for the two graphene based Pt catalysts to determine their catalytic activity for the ORR as well as for Pt/XC72 as a reference catalyst. These ORR curves with the background currents subtracted are plotted in Figure 3. From the curves, it is shown that the onset-potential of both graphene based catalysts, Pt/AG and Pt/N-AG, are very similar to that of Pt/XC72. In addition, the current density of Pt/N-AG catalyst obtained at 0.8 V is slightly higher than that of the reference catalyst (2.569 mA/cm^2 and 2.585 mA/cm^2 for Pt/XC72 and Pt/N-AG, respectively), although for Pt/AG catalyst, its current density and the limiting current were not as good as the other two curves. This could be due to the reduced conductivity by presence of defects, non-uniform distribution of Pt particles and/or the layered structure and mechanical properties of graphene hindering ORR active sites and their 3-phase reaction. Further investigation will be necessary in order to confirm the causes, however, it is evident that nitrogen doping on the activated graphene can provide a better support material to enhance the ORR performance of Pt catalyst.

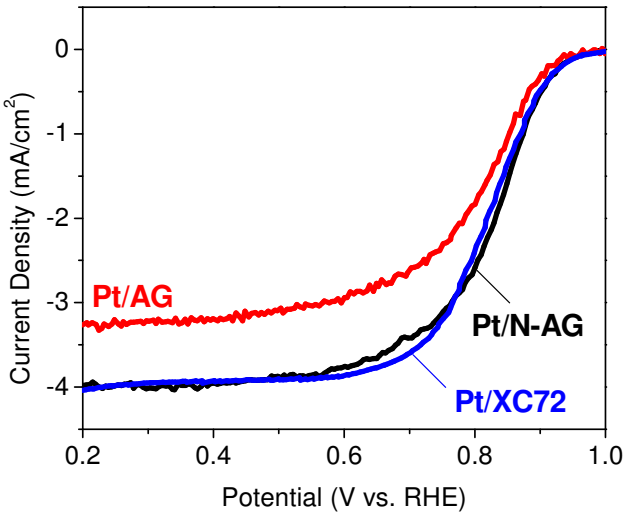

Figure 3. ORR curves of Pt catalysts supported on N-AG, AG and XC72 obtained at 900 rpm in oxygen saturated 0.1 M HClO4 electrolyte with a potential scan rate of 10 mV/s

In addition to the initial ORR performance measure, durability of the Pt/N-AG catalyst was also investigated by accelerated degradation testing (ADT) consisting of 1000 cycles in N2 saturated electrolyte at a scan rate of 50 mV/s between 0 and 1.2 V vs. RHE. Durability data of Pt/N-AG and the reference catalyst Pt/XC72 are provided in Figure 4 and their mass activities obtained at 0.8 and 0.9 V vs. RHE are listed in Table II. Pt/N-AG showed slight decrease in the limiting current and almost no evidence of degradation in the onset-potential while Pt/XC72 showed a potential decrease of 0.012 V. At 0.8 V vs. RHE, the decreases in the current densities obtained before and after ADT are 0.369 (14.2%) and 0.839 (32.64%) mA/cm^2 for Pt/N-AG and Pt/XC72 respectively, and this results in the higher percentage drop of mass activity before and after ADT for the Pt/XC72. The mass activity obtained at the same voltage drops by 29.3 % for Pt/N-AG while it is 37.5 % for Pt/XC72. This enhancement in durability is most likely arising due to the nature of graphene material such as high mechanical and chemical stability, rendering N-AG as a promising platinum catalyst support.

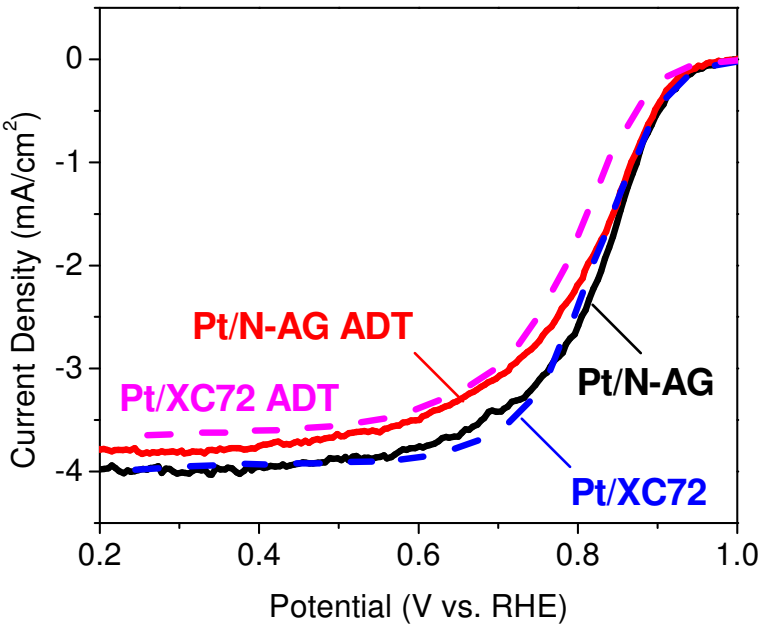

Figure 4. ORR curves of Pt/N-AG and Pt/XC72 before and after accelerated durability test obtained at 900 rpm in oxygen saturated 0.1 M HClO4 electrolyte with a potential scan rate of 10 mV/s

TABLE II. Mass activities of Pt/N-AG and Pt/XC72 catalysts before and after ADT(30, 31)

	0.9 V vs. RHE (mA/mg Pt)	**0.8 V vs. RHE (mA/mg Pt)**
Pt/N-AG	13.85	184.80
Pt/N-AG ADT	11.59	130.64
Pt/XC72	9.54	181.60
Pt/XC72 ADT	4.01	81.68

Conclusion

We have successfully synthesized a platinum nanoparticle catalyst using nitrogen-doped activated graphene as support. Well-dispersed platinum nanoparticles with controlled particle size were found on the functionalized graphene surface. This precious catalyst demonstrates promising electrocatalytic activity and durability for the ORR when compared with the commercial platinum catalyst supported on XC72, rendering graphene as a suitable replacement to traditional nanostructured carbon support materials. Among two types of graphene supports used, Pt on N-AG was found to display optimal ORR activity and durability. The high stability demonstrated through ADT is most likely due to the characteristics of nitrogen-doped graphene as a support material. Thus, graphene is presented as an ideal catalyst support material, with promising ORR activity and stability demonstrated. Future investigations will focus on characterizing the interaction among nitrogen, graphene and platinum nanoparticles as well as to apply the material in other types of fuel cell catalysts.

Acknowledgments

This research was financially supported by the Natural Sciences and Engineering Research Council of Canada (NSERC) University of Waterloo, and the Waterloo Institute for Nanotechnology.

References

1. C. W. B. Bezerra, L. Zhang, K. Lee, H. Liu, A. L. B. Marques, E. P. Marques, H. Wang and J. Zhang, *Electrochim Acta*, **53**, 4937 (2008).
2. K. Lee, L. Zhang, H. Lui, R. Hui, Z. Shi and J. Zhang, *Electrochim Acta*, **54**, 4704 (2009).
3. C. Sealy, *Materials Today*, **11**, 65 (2008).
4. L. Zhang, J. Zhang, D. P. Wilkinson and H. Wang, *J Power Sources*, **156**, 171 (2006).
5. W. Li, C. Liang, W. Zhou, J. Qiu, Zhou, G. Sun and Q. Xin, *The Journal of Physical Chemistry B*, **107**, 6292 (2003).
6. Y. Shao, J. Liu, Y. Wang and Y. Lin, *J Mater Chem*, **19**, 46 (2009).
7. E. Antolini and E. R. Gonzalez, *Solid State Ionics*, **180**, 746 (2009).
8. M. S. Saha, R. Li and X. Sun, *Electrochem Commun*, **9**, 2229 (2007).
9. X. Chen and S. S. Mao, *ChemInform*, **38**, no (2007).
10. S. H. Lee, R. Deshpande, P. A. Parilla, K. M. Jones, B. To, A. H. Mahan and A. C. Dillon, *Advanced Materials*, **18**, 763 (2006).
11. M. K. Jeon, H. Daimon, K. R. Lee, A. Nakahara and S. I. Woo, *Electrochem Commun*, **9**, 2692 (2007).
12. D. J. Ham, Y. K. Kim, S. H. Han and J. S. Lee, *Catalysis Today*, **132**, 117 (2008).
13. Z. Chen, D. Higgins, H. Tao, R. S. Hsu and Z. Chen, *The Journal of Physical Chemistry C*, **113**, 21008 (2009).
14. T. Palaniselvam, R. Kannan and S. Kurungot, *Chem Commun*, **47**, 2910 (2011).
15. J. Y. Choi, R. S. Hsu and Z. W. Chen, *J Phys Chem C*, **114**, 8048 (2010).

16. Y. Lin, X. Cui, C. Yen and C. M. Wai, *The Journal of Physical Chemistry B*, **109**, 14410 (2005).
17. X. Sun, R. Li, D. Villers, J. P. Dodelet and S. Désilets, *Chemical Physics Letters*, **379**, 99 (2003).
18. J. Guo, G. Sun, Q. Wang, G. Wang, Z. Zhou, S. Tang, L. Jiang, B. Zhou and Q. Xin, *Carbon*, **44**, 152 (2006).
19. J. Lee, J. Kim and T. Hyeon, *Advanced Materials*, **18**, 2073 (2006).
20. W. Zhang, P. Sherrell, A. I. Minett, J. M. Razal and J. Chen, *Energ Environ Sci*, **3**, 1286 (2010).
21. S. H. Joo, C. Pak, D. J. You, S.-A. Lee, H. I. Lee, J. M. Kim, H. Chang and D. Seung, *Electrochim Acta*, **52**, 1618 (2006).
22. J. B. Joo, P. Kim, W. Kim, J. Kim and J. Yi, *Catalysis Today*, **111**, 171 (2006).
23. L. Zhang, J. Niu, L. Dai and Z. Xia, *Langmuir*, **28**, 7542 (2012).
24. C. H. Choi, S. Y. Lee, S. H. Park and S. I. Woo, *Applied Catalysis B: Environmental*, **103**, 362 (2011).
25. K. Gong, F. Du, Z. Xia, M. Durstock and L. Dai, *Science*, **323**, 760 (2009).
26. A. K. Geim and K. S. Novoselov, *Nat Mater*, **6**, 183 (2007).
27. S. Yang, X. Feng, X. Wang and K. Müllen, *Angewandte Chemie*, **50**, 5339 (2011).
28. L. Qu, Y. Liu, J.-B. Baek and L. Dai, *ACS Nano*, **4**, 1321 (2010).
29. H. C. Schniepp, J.-L. Li, M. J. McAllister, H. Sai, M. Herrera-Alonso, D. H. Adamson, R. K. Prud'homme, R. Car, D. A. Saville and I. A. Aksay, *The Journal of Physical Chemistry B*, **110**, 8535 (2006).
30. F. Maillard, M. Martin, F. Gloaguen and J. M. Léger, *Electrochim Acta*, **47**, 3431 (2002).
31. G. Liu, H. Zhang and J. Hu, *Electrochem Commun*, **9**, 2643 (2007).